An investigation and design of novel moment-resisting beam-column connections for precast concrete construction

Mustafa Mahamid, Ines Torra-Bilal, and Eray Baran

- This study investigated the behavior of a moment-resisting hybrid exterior beam-column connection experimentally and numerically.
- This paper builds on previous research as part of a larger study that included three-dimensional nonlinear finite element analysis (FEA) models and experimental tests that investigated the behavior of a typical monolithic and precast concrete hybrid beam-column connection exposed to reversed cyclic loading.
- A detailed design procedure and example, which was developed based on failure modes and investigated limit states from FEA modeling and experimental results, is presented in this paper.

Precast concrete structural systems have demonstrated their cost effectiveness when compared with cast-in-place reinforced concrete and structural steel systems. This construction approach minimizes the labor-intensive aspects of production and installation and offers potential advantages such as rapid construction, enhanced quality control, and reduced overall project expenses in comparison to traditional methods. However, the use of precast concrete structural systems has primarily been limited to single-story industrial structures and nonseismic applications. This limitation stems largely from the absence of secure connection methods capable of efficiently transferring forces between beam and column components in precast concrete moment-resisting frames. In addition, the seismic performance of precast concrete structures has been relatively subpar during moderate and high-intensity earthquakes in various countries worldwide.[1,2] Notably, the vulnerability of precast concrete buildings to seismic events has been associated with inadequacies in the detailing and design of connections, as exemplified by the 1999 earthquake in Kocaeli, Turkey, and the 1994 earthquake centered in the Los Angeles, Calif., neighborhood of Northridge.

Numerous studies have delved into the performance of different types of connections in moment-resisting precast concrete frame systems. One of the most extensive experimental investigations on systems composed of precast concrete components was conducted as part of the Precast Seismic Structural Systems research program at the University of California.[3,4] According to the experimental findings, the building exhibited highly satisfactory behavior in both lateral directions, with only minor damage observed in the structural elements at a 4.0% drift level.

Other research efforts aimed at developing and testing various moment-resisting connections between precast concrete beams and columns were carried out at the University of Minnesota by French et al.[5,6] These studies drew conclusions about connection performance based on criteria such as strength and ductility.

In addition, some researchers have focused on exploring the numerical behavior of precast concrete connections. Nzabonimpa et al.[7] conducted an analytical investigation of a novel mechanical beam-column connection integrated into precast concrete moment frames. Their study revealed that the nonlinear finite element analysis (FEA) approach yielded results that were in good agreement with experimental data, enabling the examination of beam end plate deformations and concrete damage at the joint region. In a separate study, Najafgholipour et al.[8] performed numerical simulations of reinforced concrete joints subjected to simulated lateral loads, with a specific focus on assessing shear behavior at the beam-column connection area. This research scrutinized the shear capacity of the joint and the resulting deformation patterns.

The goal of the study described in this article was to investigate the behavior of a moment-resisting hybrid exterior beam-column connection experimentally and numerically and develop a connection design procedure based on failure modes and investigated limit states. Three-dimensional (3-D) nonlinear FEA models were developed for a typical monolithic beam-column connection and a precast concrete hybrid beam-column connection using the FEA software Abaqus. The connection models were exposed to reversed cyclic loading and the results were compared with experimental data. FEA results show good agreement with experimental results, suggesting that computational models present an attractive and cost-efficient alternative to experiments. A detailed design procedure was developed as an outcome of this study.

Description of connections

A previous, extensive experimental investigation was conducted to test exterior reference monolithic and novel precast concrete beam-column connections.[9] The experimental study focused on the connection configurations and modification to predict optimized performance under cyclic loading. A total of 13 connections (2 monolithic and 11 precast concrete specimens with various detailing schemes) were investigated to better understand their behavior.[9] For the sake of brevity, results for only one typical monolithic connection and one precast concrete connection are provided in this article. **Figure 1** shows the geometric details and reinforcement arrangements for the monolithic and precast concrete specimens.

As part of the beam-column joint assembly, column elements featuring a standard cross section measuring 400 × 400 mm (16 × 16 in.) were used. These columns were constructed with 12 longitudinal reinforcing bars, each having a diameter of 20 mm (0.79 in.), along with 8 mm (0.3 in.) diameter stirrups spaced at 100 mm (4 in.). The test specimens were constructed using a typical column height of 1410 mm (55.5 in.).

The beam elements had a rectangular cross section measuring 400 × 250 mm (16 × 10 in.) and a length of 1800 mm (71 in.). These beams were reinforced symmetrically at both the top and bottom with six 20 mm (0.79 in.) diameter or 16 mm (0.6 in.) diameter longitudinal bars. The yield strengths of the 16 and 20 mm diameter reinforcing bars were 525 and 465 MPa (76.1 and 67.4 ksi), respectively.

The reference specimen for evaluating the performance of the investigated precast concrete beam-column connection details was the monolithic specimen. To facilitate the transfer of forces between the beam and column elements within the precast concrete connections, L120 × 120 × 12 (L5 × 5 × ½) steel angles measuring 400 mm (16 in.) in length were used both at the top and bottom of the connection. These steel angles were affixed to the column face using 30 mm (1.2 in.) diameter steel threaded rods, which were preloaded to a 30 kN (6.7 kip) load level. The threaded rods had measured yield and ultimate strengths of 458 and 517 MPa (66.4 and 75.0 ksi), respectively. Inside the beam element, embedded steel plates with dimensions of 120 mm (5 in.) in width, 12 mm (0.5 in.) in thickness, and 250 mm (10 in.) in length were securely anchored. Steel top and bottom angles were welded to these plates to establish force transfer between the beam and column components. The specified minimum yield strengths for the steel plates and the angles were 235 MPa (34 ksi) using Grade S235 steel and 275 MPa (40 ksi) using Grade S275 steel, respectively. **Figure 2** illustrates the details of the connection region within the precast concrete beam elements. In Specimen D1, three 16 mm (0.6 in.) diameter Z-shaped steel reinforcing bars, each with a total length of 600 mm (24 in.), were welded to each embedded steel plate. The Specimen D1 concrete had a compressive strength of 32.7 MPa (4.74 ksi). Additional connection modifications and configurations, including U-shaped bars, vertical plates, vertical bars, UPN steel sections, and others, underwent experimental testing, with the corresponding results documented in previously published studies by the same authors.[9,10]

Figure 3 shows the testing framework designed for conducting load tests on the specimens. The figure provides information on the overall dimensions of the specimens and the specific connection geometry. The column specimen was affixed to a steel frame using pin connections at both the top and bottom; the aim was to constrain vertical and horizontal displacements. The distance between these two pins was set at 1900 mm (75 in.). To apply the load, a hydraulic cylinder with a 500 kN (112 kip) capacity was positioned 1800 mm (71 in.) from the face of the column near the free end of the beam. Displacement-controlled reversed cyclic loading was used

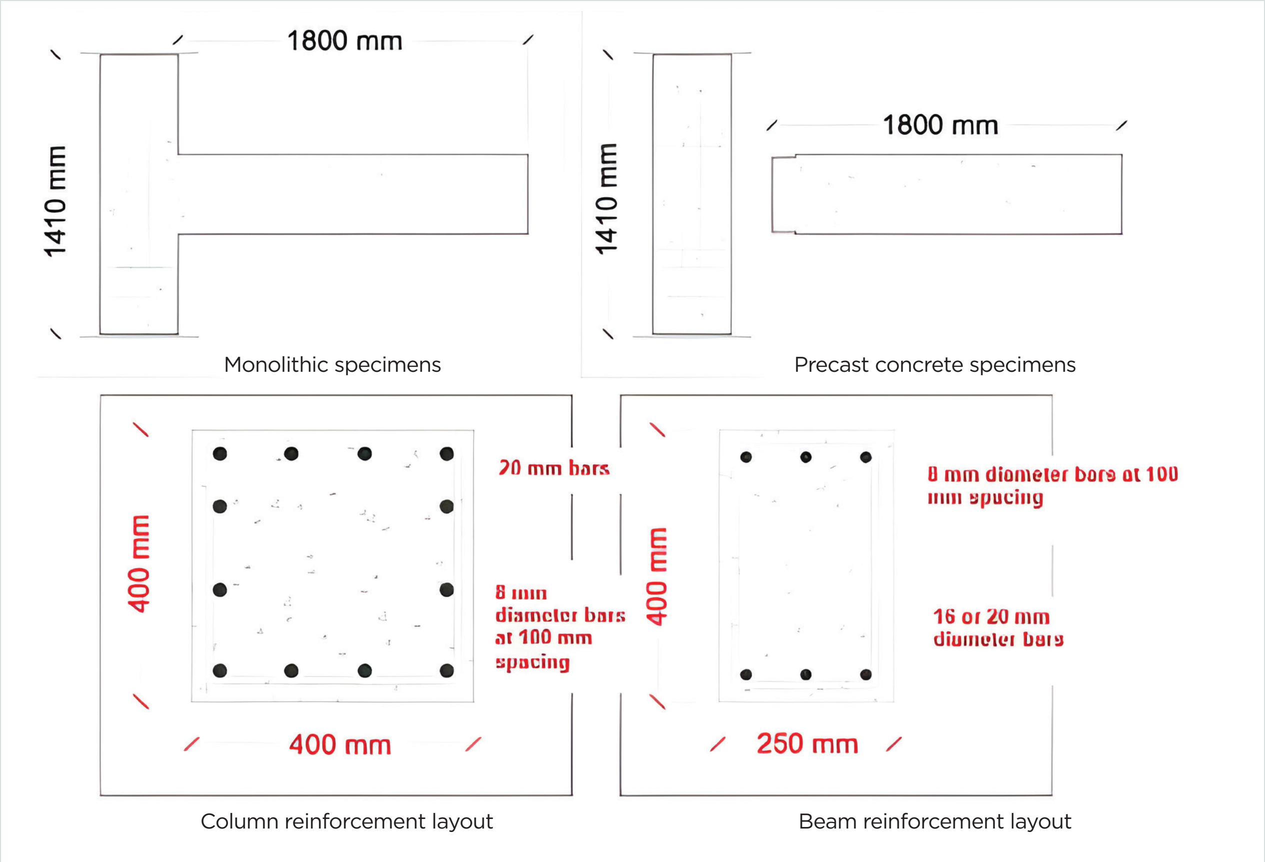

Figure 1. Geometry of test specimens. Note: 1 mm = 0.0394 in.

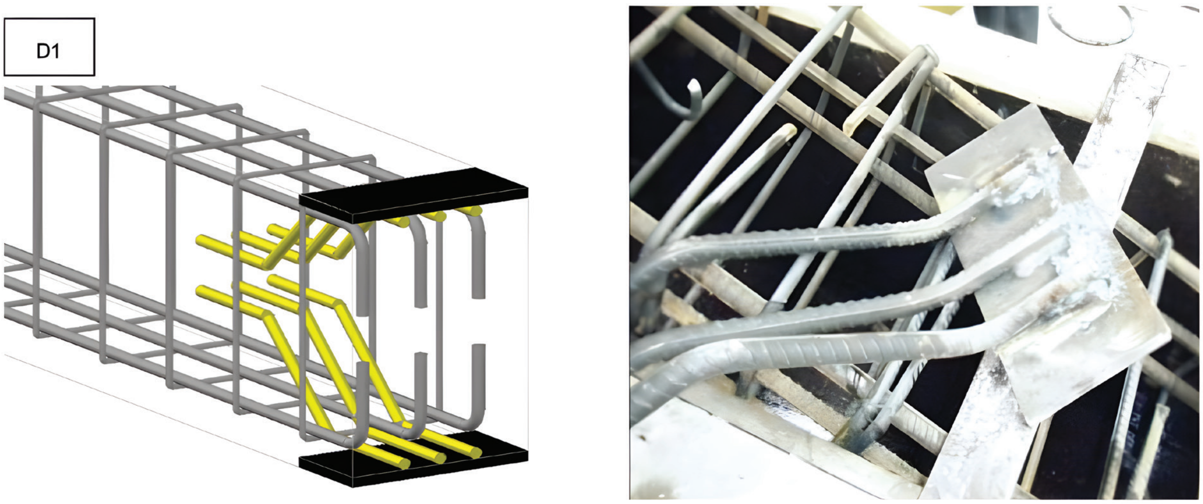

Figure 2. Reinforcement detailing schemes in connection region D1.

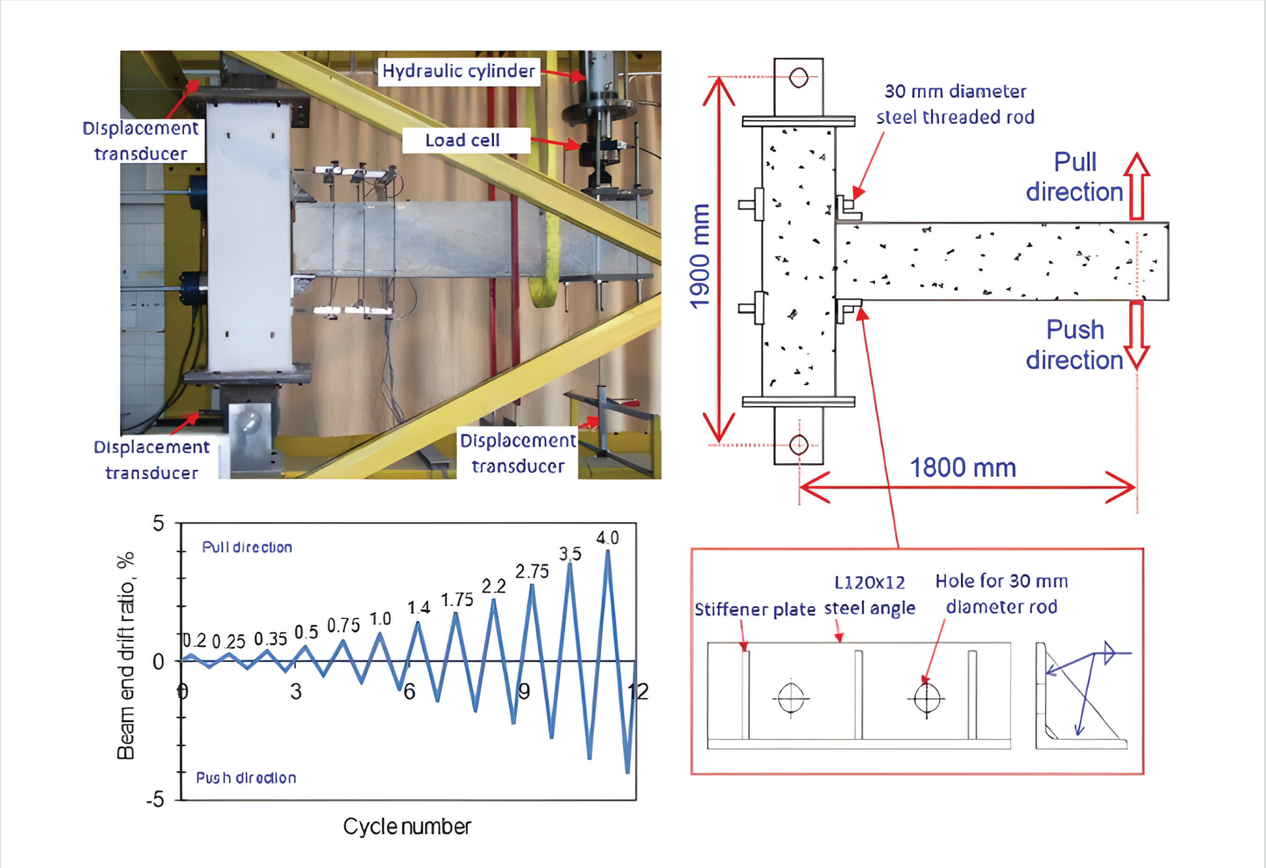

Figure 3. Specimen details, test setup, and applied loading.
Note: L120 × 12 = L120 × 120 × 12 = L5 × 5 × ½; 1 mm = 0.0394 in.

for the testing, with incremental displacement amplitudes adhering to the guidelines outlined in the American Concrete Institute's (ACI's) *Acceptance Criteria for Moment Frames Based on Structural Testing* (ACI 374.1)[11] (Fig. 3). For more comprehensive insights into the loading mechanism, construction procedures for the beam-column connection, and the force transfer mechanism of the connection components, refer to Baran et al.[9]

FEA modeling approach

In a previous study, extensive nonlinear FEA of monolithic and precast concrete beam-column connections were performed using Abaqus software.[10] This previous study contributed to the overall novelty of the investigation by presenting a calibrated and refined modeling approach to capture the accurate behavior of these connections. For the study presented in this article, numerical results were shown for only one typical monolithic and one precast concrete connection to prove the validity of the proposed FEA approach. A more detailed description of the FEA approach is available in the previously published study.[10]

The entire model, including concrete, steel reinforcement, and other steel components, used 3-D eight-node reduced integration brick elements with hourglass control, known as C3D8R in the Abaqus library. This choice was made to realistically capture the behavior of reinforcement under cyclic loading and accurately identify all potential failure modes of the reinforcement across multiple load cycles. To model connections similar to those investigated in this study, the primary challenge involves simulating the intricate behavior of reinforced concrete structures subjected to simulated cyclic loading. The FEA of the investigated connections was conducted through a nonlinear static analysis method, with cyclic loading applied in a displacement-controlled manner, divided into several load increments. To enhance the accuracy of the numerical model, a modified concrete damage plasticity (CDP) model was incorporated. The CDP model simulates concrete behavior while considering the softening effect observed in cracked concrete under cyclic loading. This approach considers both the compression-softening effect and the tension-stiffening effect in reinforced concrete. **Figures 4** and **5** depict typical softened damage plasticity curves for compression and tension, respectively. Furthermore, damage is defined for both uniaxial tension and compression during the softening phase in the CDP model. The degradation of elastic stiffness in the softening regimen is characterized by two damage variables—namely, d_t for tensile damage and d_c for compressive damage—both of which were integrated into the numerical model.[10]

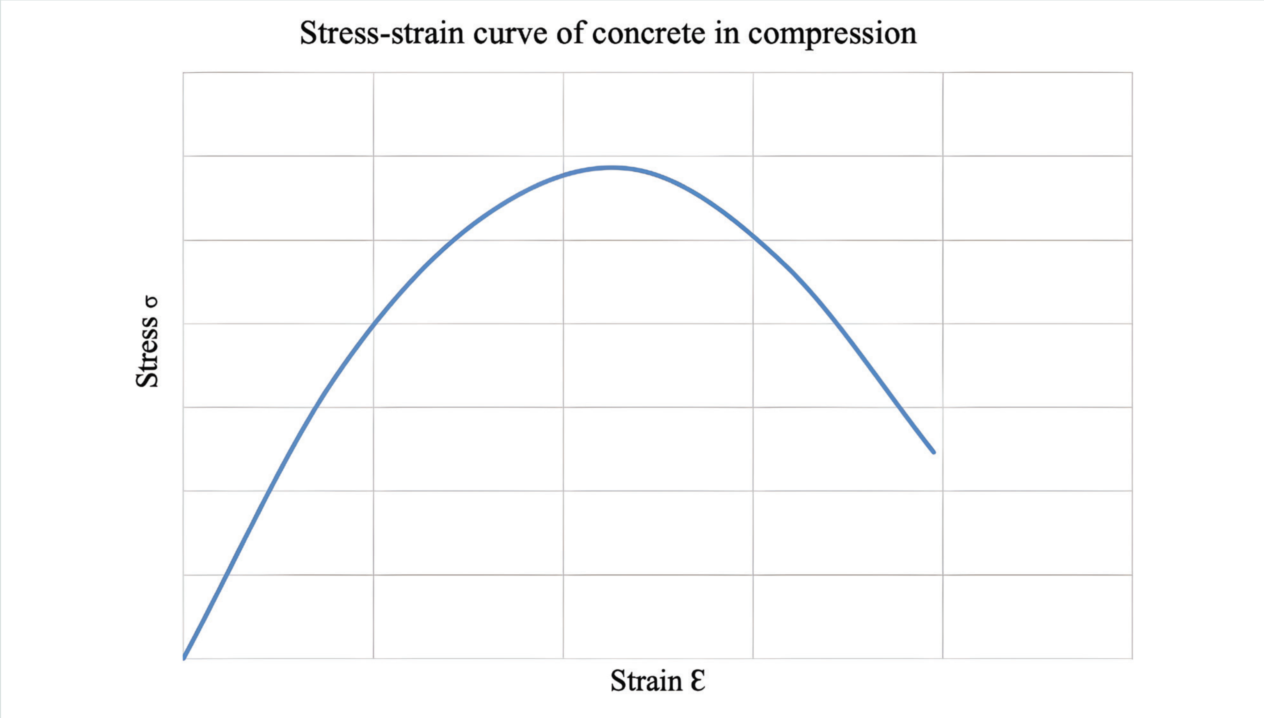

Figure 4. Typical stress-strain relationship for concrete in compression with compression-softening effect.

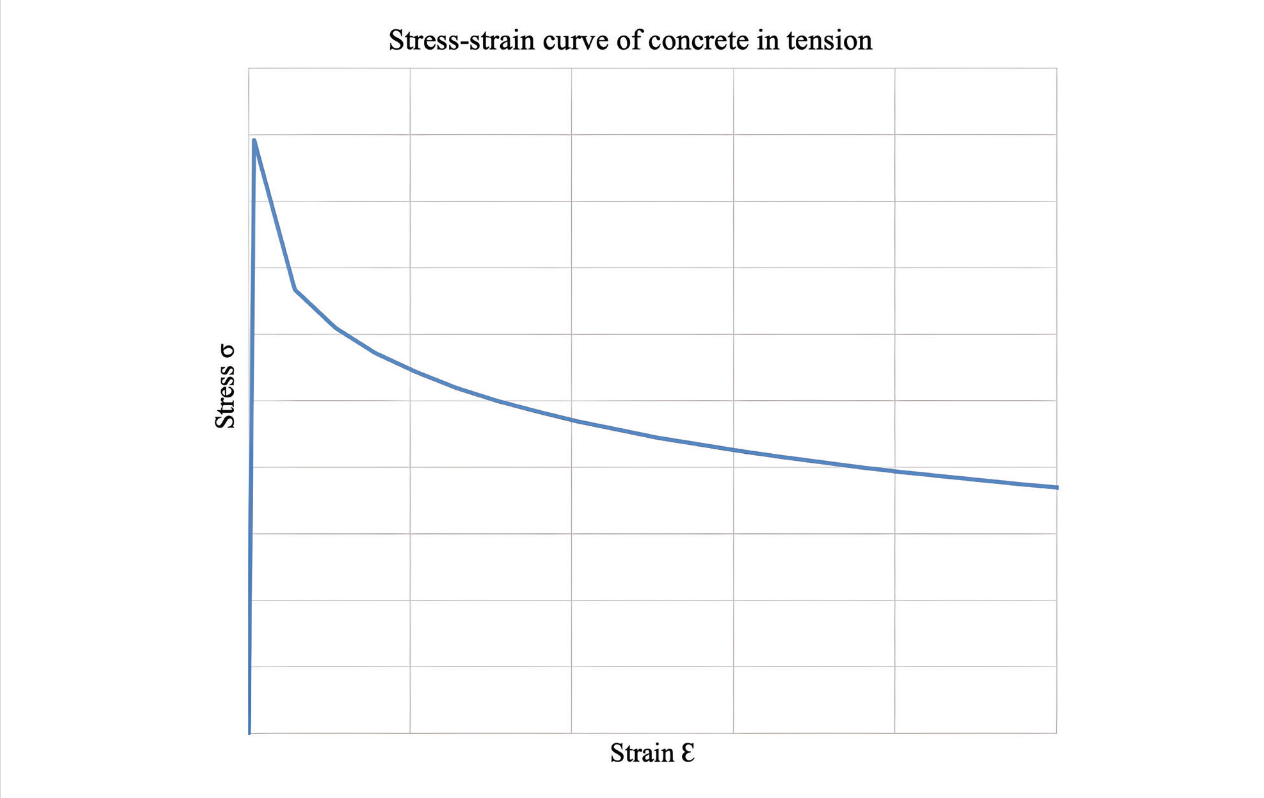

Figure 5. Typical stress-strain relationship for concrete in tension with tension-stiffening effect.

Bilinear constitutive relationship was used to model the steel components. The von Mises yield criterion was used to predict yielding in steel material. The behavior after the yield point follows the kinematic strain-hardening rule, which represents the real material behavior for cyclically loaded materials. **Figure 6** shows the typical stress-strain curve used for steel components.

An important factor considered in this study was the bond-slip effect of the steel reinforcement, which highly influences the behavior of the beam-to-column connections subjected to cyclic loadings. This effect is particularly significant in the joint and plastic hinge regions because the reinforcing bars in these regions tend to undergo large bond-slip actions, and assuming a perfect bond would not be accurate.

Surface-to-surface interaction was used between the steel angle and column as well as between the steel rods and the angles. Tie constraint was used to define the interaction between the steel angles and the beam to ensure complete transfer of the load. The embedded region command with bond-slip effect was used to simulate the interactions of all reinforcement bars with the beam and column. The boundary conditions and loading were applied to all investigated specimens in a manner similar to the experiments. The beam end was free to rotate in all directions and free to move laterally in the x and z directions. A set of nodes was defined at the beam top edge, which was tied to a reference point through a rigid body connection. The reversed cyclic loading was applied in the y direction at the defined reference point. In addition, self-weight was added as a gravity load to the model. All parts were selected as dependent parts to perform meshing at a part level, and part partitioning was used. Mesh convergence was achieved by decreasing the element size and analyzing the impact of this process on the accuracy of the solution. A calibrated average mesh size of 35 mm (1.4 in.) was used to model concrete and steel parts. **Figure 7** shows the meshed concrete model and steel parts including the reinforcement. Pretensioning of the steel rods performed in the experimental testing was added to the numerical model as bolt loads."

FEA results

Figure 8 compares the force-displacement curves obtained from FEA simulations and experimental findings for the monolithic connection M and precast concrete connection D1. As the plots illustrate, the hysteresis curves predicted through numerical analysis closely align with the observed responses for both the monolithic and the precast concrete connection. Remarkably, there is a notable concordance

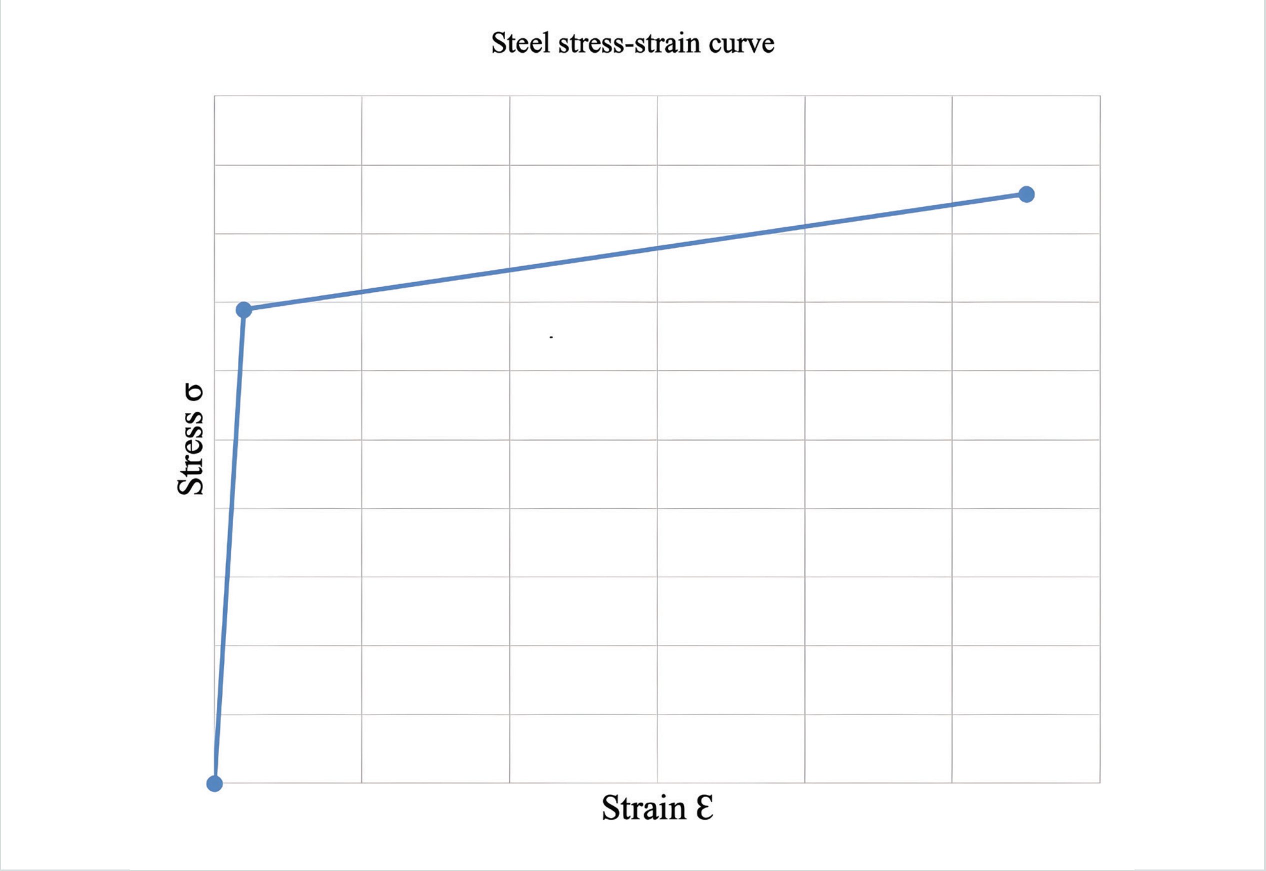

Figure 6. Typical steel stress-strain curve.

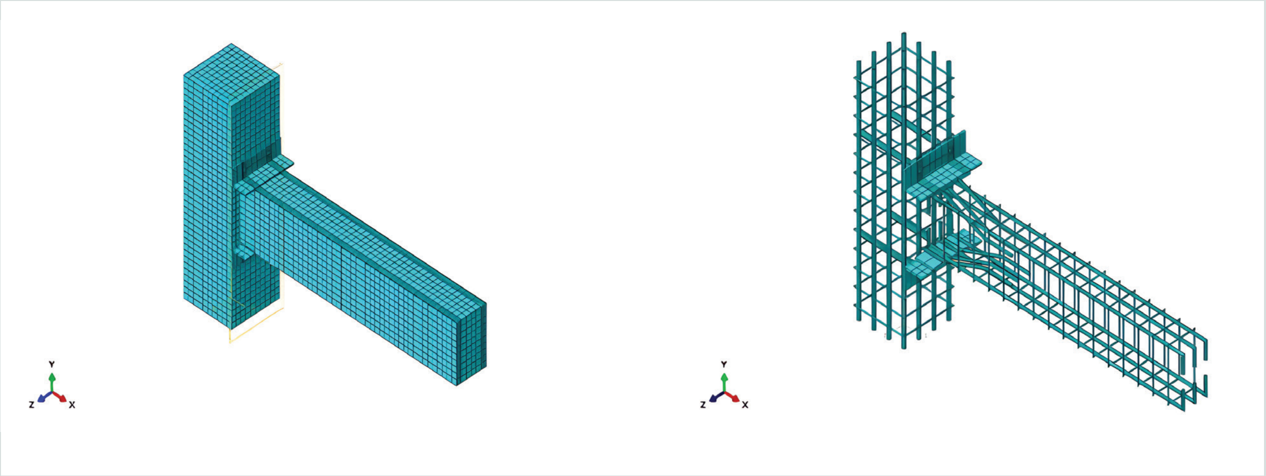

Figure 7. Meshed finite element analysis model showing concrete and steel components.

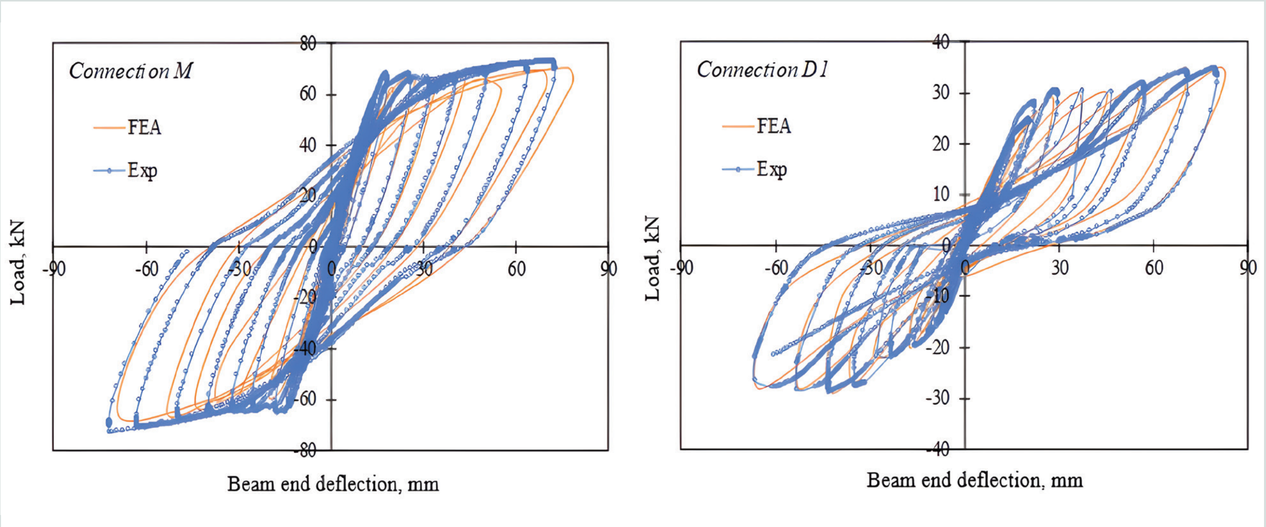

Figure 8. Comparison of measured and predicted load-deflection responses. Note: Exp = experimental testing; FEA = finite element analysis. 1 mm = 0.0394 in.; 1 kN = 0.225 kip.

between the numerical and measured behavior, particularly regarding the maximum force levels achieved during each drift cycle. Furthermore, the FEA results effectively capture the pinching behavior observed in the precast concrete connection.

The performance of the FEA was examined across various load cycles and then contrasted with the failure modes observed in the experimental data. In general, both the FEA and the experiments exhibited a common primary failure mode in the concrete. In addition, the FEA managed to identify additional failure modes associated with the steel components. **Figures 9** and **10** depict some of these failure modes as predicted by the FEA for the monolithic connection and precast concrete connections.

Stiffness degradation curves were formulated based on the FEA outcomes and were subsequently juxtaposed with the experimental findings across various load cycles, encompassing both the monolithic and precast concrete connections under investigation. To derive the stiffness of the specimens in each loading cycle, the slope of the line connecting the maximum drift points in both pull and push directions was calculated. The variation of stiffness degradation was consistent between the experimental and FEA results for both connections (**Fig. 11**). The percentage difference falls within acceptable margins and is primarily attributable to minor distinctions in the hysteresis results for both types of connections. In congruence with the experimental results, both the monolithic and precast concrete connections exhibited stiffness degradation as the beam-end drift ratio

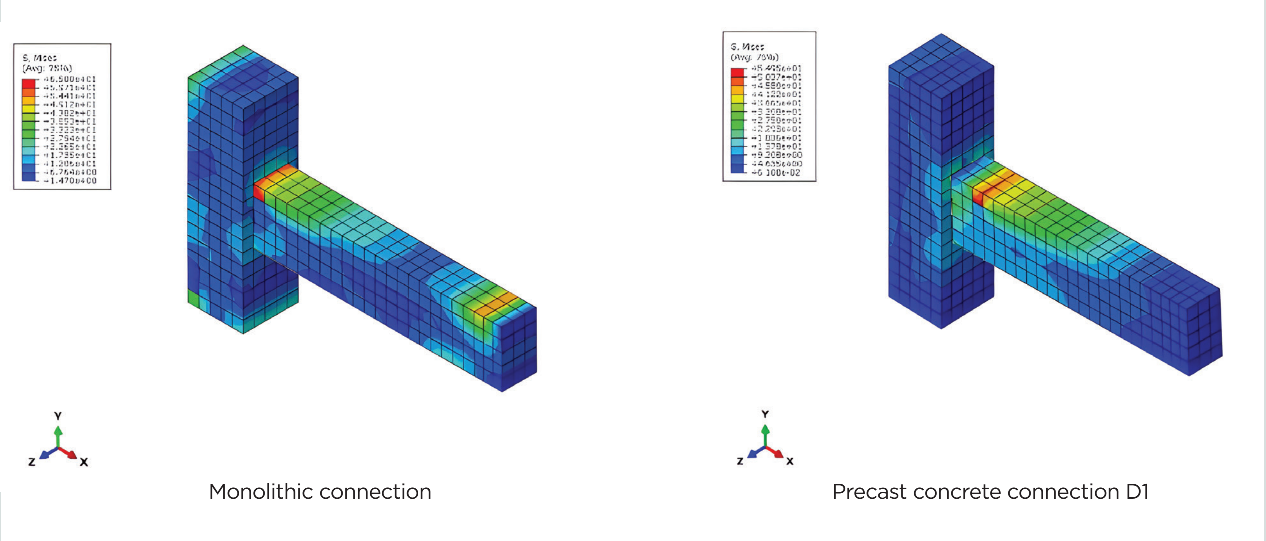

Figure 9. Finite element analysis model representation of concrete failure in the connections at 4% beam drift ratio.

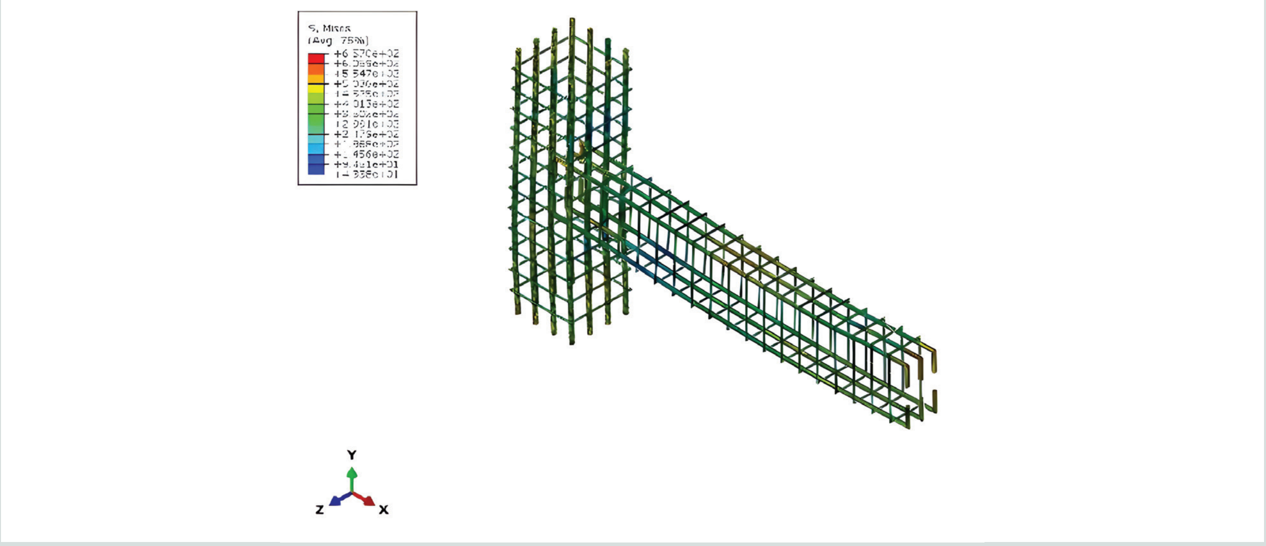

Figure 10. Finite element analysis model representation yielding in the longitudinal bars of precast concrete connection D1 at 4% beam drift ratio.

increased. Notably, both numerical and measured responses indicate a heightened rate of degradation occurring during the earlier drift cycles.

Figure 12 shows the comparison of the numerically predicted energy dissipation response for the examined monolithic and precast concrete connections with the observed results. To compute the energy dissipated during each loading cycle, we calculated the area enclosed by the hysteresis loop. Subsequently, the sum of the dissipated energy calculated for each cycle was calculated to obtain the cumulative dissipated energy. Figure 12 shows that a satisfactory level of validation was achieved between the FEA and experimental outcomes in terms of dissipated energy at various cycles. Notably, the agreement between the FEA and experimental results is more pronounced for the precast concrete connection than for the monolithic one. This observation aligns with expectations because most of the energy dissipation occurs at higher beam-end drift ratios, subsequent to the onset of damage. It is worth noting that, as part of this research, alternative connection details were proposed to enhance the energy dissipation mechanism of precast concrete connections. However, these proposals fall outside the scope of the specific study being discussed here.

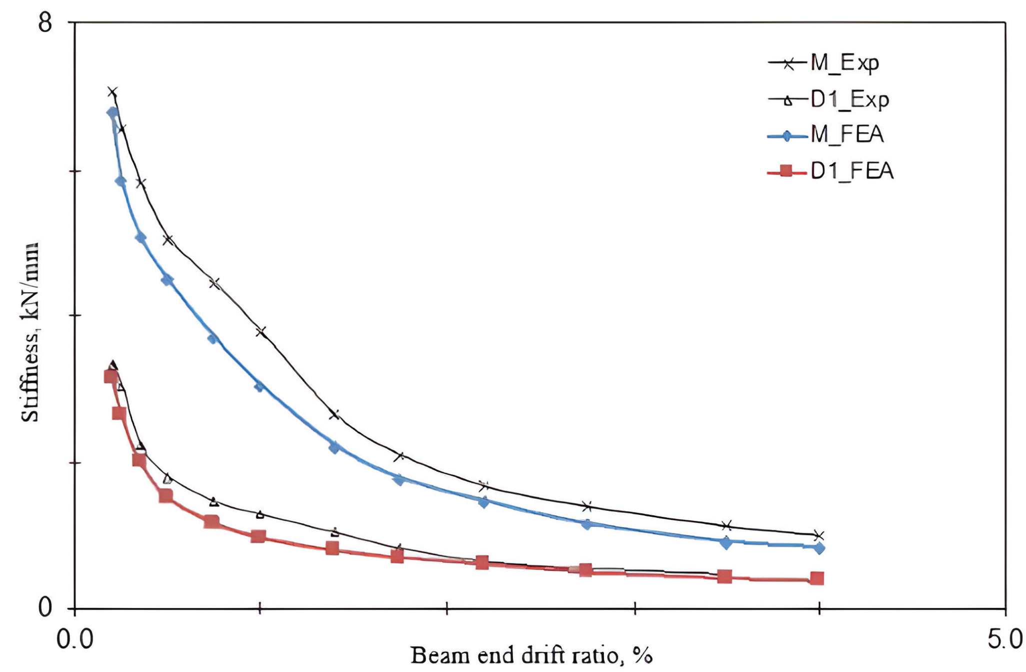

Figure 11. Comparison of measured and predicted stiffness degradation. Note: D1_Exp = experimental values for precast concrete connection D1; D1_FEA = finite element analysis values for precast concrete connection D1; M_Exp = experimental values for monolithic connection M; M_FEA = finite element analysis values for monolithic connection M. 1 kN/mm = 5.71 kip/in.

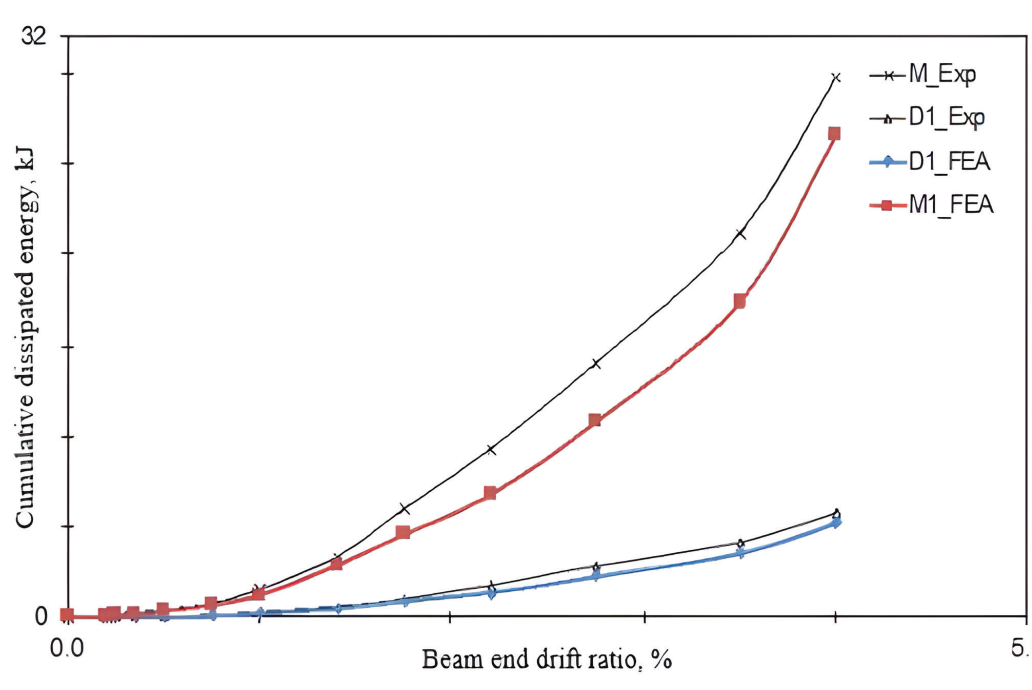

Figure 12. Comparison of measured and predicted cumulative dissipated energy. Note: D1_Exp = experimental values for precast concrete connection D1; D1_FEA = finite element analysis values for precast concrete connection D1; M_Exp = experimental values for monolithic connection M; M1_FEA = finite element analysis values for monolithic connection M1.

According to the FEA results, concrete cracking emerged as a prominent failure mode in the early stages of loading for the monolithic connection. In addition, the yielding of longitudinal steel bars and stirrups occurred prematurely in the monolithic connection. Both experimental observations and FEA simulations reveal a distributed form of damage characterized by concrete cracking in both the beam and column elements of this monolithic specimen. In contrast, the investigated precast concrete connection, designated as D1, displayed a different pattern of damage. In this case, the damage was primarily localized in the connecting steel angles and anchorage bars. Concrete failure was delayed until a later load cycle, occurring at a higher beam-end drift ratio (2.2%) than in the monolithic connection (0.5%). Most of the damage was concentrated in the beam element, with minimal damage observed on the column element. This outcome was attributed to the proposed connection detailing method, which seems to delay concrete damage and prevent the formation of plastic hinges on the column. Such behavior may be preferred in practice. Overall, the FEA contributed to a deeper understanding of the potential performance of a typical precast concrete connection when compared with a conventional monolithic connection.

Design of precast concrete seismic connections

Proposed design procedure

An important contribution of this study is a proposed design procedure for the investigated precast concrete connections under cyclic loading. Precast concrete connections with various unique construction details were investigated to determine their capacity. The embedded steel components highly influenced the overall capacity of the connections, and it was previously concluded that minor detailing modifications greatly affect the performance of the connections.

The basis of the proposed design procedure includes the following:

- The beam-column connection region is considered to be the location of the maximum seismic forces and applies to multistory columns with single bay beams.
- Ductile connections developed for this application result in yielding of the connection components at the beam-column interface, with less damage to the precast concrete beam and column elements.
- Adequate concrete confinement shall be provided at the beam end near the connection region by providing stirrups, with the size and spacing as required by ACI's *Building Code Requirements for Structural Concrete (ACI 318-19) and Commentary (ACI 318-19R)*.[12]
- Beam longitudinal bars along with additional Z-shaped bars provide most of the flexural strength and energy dissipation.
- To ensure substantial shear strength, the vertical shear resistance of the beam element in the connection region is provided by geometric constraints (as will be presented in the following design steps), and by reduced stirrup spacing compared with the rest of the beam length away from the connection region. An additional shear capacity check is performed to verify the resistance against shear demands due to seismic and nonseismic effects.
- Column design is not included in detail as part of this procedure. The column design shall satisfy capacity design requirements of a typical reinforced column per ACI 318-19[12] and ACI 550.3-13.[13]
- An overstrength factor of 3 is applied to seismic design of anchor rods for maximum tension as specified in ACI 318-19 section 17.10.5.3 (d) and Table 12.2-1 of the American Society of Civil Engineers' *Minimum Design Loads and Associated Criteria for Buildings and Other Structures*, ASCE 7-16.[14]

The proposed design procedure is intended to ensure that the proposed connections can accommodate required drift demands by taking into account the following performance requirements:

- The reinforcing steel shall yield but must not fracture before reaching the required drift demand.
- The steel angles may yield and deform, but the connection rods shall be designed to remain elastic under tensile forces, including prying effects resulting from angle deformation.

To propose a design procedure for these connections, we have made the following assumptions:

- The design force effects and loadings (design moment due to applied loading (gravity and earthquake loading) creating tension at top face of beam M_{des_top}, design moment creating tension at bottom face of beam [earthquake loading only] M_{des_bot}, applied dead loading w_D, and applied live loading w_L) and maximum design drift ratio θ_{des} are known from analysis.
- Maximum pull and push forces are known from analysis or experiments.
- The column and beam dimensions, including span length and column height, are known from the building layout.
- The cross sections of the frame members are known from initial assumptions.
- Material properties are known.

The following steps shall be followed for the design of precast concrete connections consisting of single angles attached to the column face at top and bottom of the beam.

1. Define material properties of hybrid frame components, including the following:

- concrete compressive strength f_c'
- steel reinforcement yield stress f_y, modulus of elasticity E_s, and tensile strength f_u
- overstrength factors for compression and tension steel reinforcement and connection (anchor) rods Ω_c, Ω_t, and Ω_b, respectively
- tensile strength for connection (anchor) rods F_{nt}

2. Obtain design force effects and loads M_{des_top}, M_{des_bot}, w_D, and w_L and drifts θ_{des}. (Design loads can be obtained using various analysis software.)

3. Define frame dimensions.

   a. Check the beam span-to-depth ratio per ACI 318-19 section 18.6.2.1(a).
   The minimum clear span to depth ratio shall be greater than 4 to ensure that no slip occurs between beam and column. This requirement also ensures that the vertical shear at the beam-column interface induced by seismic deformations can be resisted by the moment induced compression force.

   $$\frac{L_{clear}}{h} > 4$$

   where

   h = beam height

   L_{clear} = clear span of beam between column faces

   b. Check whether the beam depth is smaller than one-third of the clear span of beam between column faces.[15]

   $$\frac{L_{clear}}{3} > h$$

   c. Check whether the beam width bb is at least greater than the lesser of 30% of beam height and 25 cm (10 in.). (ACI 318-19 section 18.6.2.1[b].)

   $$b_b \geq MIN(0.3\text{h, 25 cm})$$

   d. Estimate the required areas of steel reinforcement in tension $A_{s,req}$ and compression $A'_{s,req}$, and determine whether the provided areas of steel reinforcement in tension As and compression A'_s are greater than the required values.

   $$A_s \geq A_{s,req} = \frac{M_{des}^{+}}{0.9hf_y}$$

   $$A'_s \geq A'_{s,req} = \frac{M_{des}^{-}}{0.9hf_y}$$

4. Check that the selected reinforcement satisfies the minimum and maximum reinforcement requirements of ACI 318-19 section 18.6.3.1.

$$\rho_{reinf} \leq 0.025$$

$$A_s \geq \frac{200b_b d_b}{f_y}$$

where

ρ_{reinf} = reinforcement ratio

d_{bm} = beam depth

5. Calculate the internal forces at maximum drift ratio. The tension and compression steel may include any longitudinal bars used as part of the connection reinforcement.

$$T_s = A_s f_y$$

$$C_s = A'_s f_y$$

where

T_s = tension steel force

C_s = compression steel force

6. Determine the factor β_1 relating the depth of equivalent compressive stress block to depth of neutral axis per ACI 318-19 Table 22.2.2.4.3.

7. Compute the concrete compression force C_c in terms of the neutral axis depth c.
$$C_c = 0.85 f_c' \beta_1 b_b c$$

8. Compute neutral axis depth c and the stress block depth a.

$$c = \frac{T}{0.85 f_c' b_b \beta_1}$$

$$a = \beta_{1c}$$

9. Compute the positive and negative nominal moment capacity M_n^{+} and M_n^{-} by taking moments about the tension and compression reinforcement location.

$$M_n^{+} = T\left(d_b - \frac{a}{2}\right)$$

$$M_n^{-} = C_c\left(d_b - \frac{a}{2}\right)$$

10. Check whether the ultimate moment capacity is greater than or equal to the design moment.
$$\phi M_n^{+} \geq M_{des_{top}}$$

$$\phi M_n^{-} \geq M_{des_{bot}}$$

where

ϕ = strength reduction factor = 0.9 per ACI 318-19 Table 21.2.1

If the ultimate moment capacity (strength reduction factor times the nominal moment capacity ϕM_n) is less than or equal to the design moment M_{des}, increase the area of steel or modify the member dimensions.

11. Determine the net tensile strain in the extreme layer of longitudinal tension reinforcement ε_t, verify that the section is tension controlled per ACI 318-19 Table 21.2.2, and verify that the net tensile strain at nominal strength is greater than or equal to 0.004 per ACI 318-19 section 9.3.3.1.

$$\varepsilon_t = 0.003\left(\frac{d_b}{c} - 1\right)$$

$$\varepsilon_t \geq 0.004$$

12. Calculate shear demands dependent on gravity loads acting on the beam due to dead load w_D and live load w_L as well as seismic-induced moments for opposite ends of the precast concrete beams M_{pr1} and M_{pr2} per ACI 318-19 Fig. R18.6.5 using $1.25f_y$.

$$V_u = \frac{w_u L_{clear}}{2} + \frac{M_{pr1} + M_{pr2}}{L_{clear}}$$

$$w_u = (1.2 + 0.2S_{Ds})D + 1.0L + 0.2S$$

where

w_u = applied factored load

S_{Ds} = 5% damped, spectral response acceleration parameter at short periods per the general building code

D = service dead load

L = service live load

S = service snow load

13. Calculate and check whether shear capacity at the beam-column interface is sufficient for the shear demands. The total shear force is resisted by two separate mechanisms: the weld acting in shear at the top of the beam (resistance defined by the American Institute of Steel Construction's [AISC's] *Steel Construction Manual* section J2.4) and the anchor rods at the column acting in tension (resistance defined by AISC part 16 Table J3.2).[15]

$$\phi V_{n_{weld}} = \phi_1\left(R_{n_{weld}}\right)$$

$$\phi V_{n_{anch}} = n_{anch} \times \phi_2\left(R_{n_{anch}}\right)$$

$$\phi V_{n_{weld}} \geq V_u$$

$$\phi V_{n_{anch}} \geq V_u$$

where

n_{anch} = number of anchors resisting shear at the beam-column interface

$R_{n_{anch}}$ = anchor rods strength

$R_{n_{weld}}$ = weld strength

$V_{n_{anch}}$ = nominal shear capacity of the connection (anchor) rods

$V_{n_{weld}}$ = nominal shear capacity of the weld

V_u = maximum applied shear

ϕ_1 = strength reduction factor for weld in shear = 0.75 per ACI 318-19 Table 17.5.3(a)

ϕ_2 = strength reduction factor for anchor rod in tension = 0.75 per AISC 360-16 Table J2.5

14. Select a trial angle size t_{angle} and check the applicable limit states (tensile yielding and shear yielding) per AISC provisions.

15. Select a trial diameter for connection rods d_b.

16. Using Eq. (9-20) from the fourteenth or later edition of the AISC *Steel Construction Manual*[15] and its parameters as described in detail in part 9 of that manual, check how the provided angle thickness compares with the minimum thickness required to avoid the generation of prying forces.

$$t_{min} = \sqrt{\frac{4Tb'}{\rho F_u}}$$

where

b' = b – angle geometrical parameter as defined in AISC *Steel Construction Manual*[15] Eq. (9-21)

b = distance from bolt centerline to centerline of angle leg

d_b = bolt diameter

F_u = specified tensile strength of angle

t_{min} = angle thickness required to eliminate prying action

T = required strength/bolt

ρ = min (2(b), s), tributary length as described in the AISC *Steel Construction Manual*[15] Eq. (9-21)

s = bolt spacing

If the angle thickness is satisfactory ($t_{min} \le t_{angle}$ where tangle is the provided angle thickness), no further check for prying action is necessary. In this case, there shall be no additional force in the bolt due to prying action q, and the bolts shall be designed for maximum applied tensile forces T_u. Otherwise, calculate prying forces per Eq. (9-28) in the AISC *Steel Construction Manual*[15] and design bolts for total forces $Tu + q$.

$$q = B\left[\delta\alpha\rho\left(\frac{t}{t_c}\right)^2\right]$$

where

B = available tension per bolt

t = angle thickness as provided

t_c = angle thickness required to develop the available strength of the bolt, with no prying action

α = ratio of the moment at the center of the angle leg thickness to the moment at the bolt line

δ = ratio of net length at bolt line to gross length at the face of the leg of angle

17. Check whether rod tensile capacity is sufficient for applied loads.

$$\phi A_b F_{nt} \ge \Omega_b (T_u + q)$$

where

A_b = anchor rod area

ϕ = 0.75 per ACI 318-19 Table 17.5.3(a)

18. Check welding according to AISC part 16 section J3.2.

Summary of proposed design procedure

The flowchart in **Fig. 13** summarizes the proposed design procedure and a design example is presented in the following section. The input parameters needed for the proposed design procedure of investigated precast concrete connections under cyclic loading are defined in the notation section.

Design example

Design the beam-column connection of the precast concrete moment-resisting hybrid frame exposed to seismic loading, with the connection consisting of bolted single angles at the face of the column. The following information is given about the building layout and loading results obtained from analysis.

- Three-story office building in Chicago, Ill.
- Single bay of 15 ft (4.6 m) span length
- 10 ft (3 m) story height
- M_{des_EQ} = maximum design moment due to earthquake load and gravity based on a drift ratio θ_{des} of 2% = 200 kip-ft (270 kN-m)
- M_{des_DL} = maximum design moment due to gravity based on a drift ratio θ_{des} of 2% = 300 kip-ft (407 kN-m)
- w_D = 2.5 kip/ft (36.5 kN/m)
- w_L = 1.7 kip/ft (24.8 kN/m)
- F_{pull} = maximum pull force at beam tip used to obtain tension in the anchors from combined gravity and lateral forces at 2% drift = 8.51 kip (37.9 kN)
- F_{push} = maximum push force at beam tip used to obtain tension in the anchors from combined gravity and lateral forces at 2% drift= 7.82 kip (34.8 kN)

1. Establish material properties.

   f'_c = 4 ksi (27.6 MPa)

   E_s = 29,000 ksi (200 GPa)

   f_y = 60 ksi (414 MPa)

   F_u = 75 ksi (517 MPa)

   F_{nt} = 90 ksi (621 MPa)

   Ω_b = 3

2. Design loads (M_{des_DL}, M_{des_EQ}, w_D, w_L, F_{pull}, F_{push}) were provided from analysis results.

3. Assume the dimensions of the sections and verify that they meet the previously mentioned requirements.

   h = 30 in. (762 mm)

   d_b = 27.5 in. (698.5 mm)

   b_b = 16 in. (406 mm)

   d_c = column depth = 24 in. (610 mm)

   b_c = column width = 24 in.

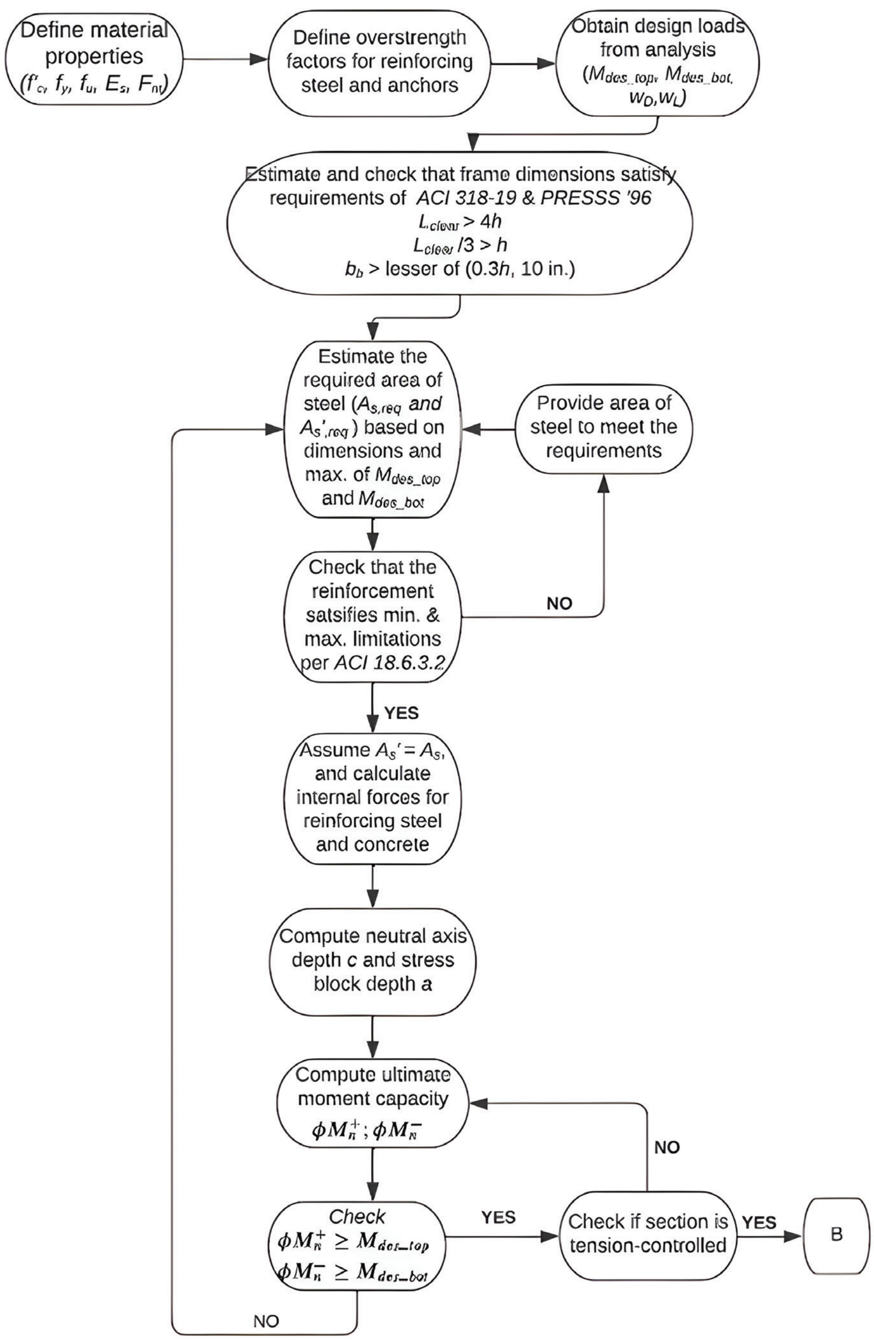

Figure 13. Design procedure flowchart. Note: a = stress block depth; A_b = anchor rod area; ACI = *Building Code Requirements for Structural Concrete (ACI 318-19) and Commentary (ACI 318-19R)*; AISC = American Institute of Steel Construction's *Steel Construction Manual* (2010); A_s = provided area of steel in tension; A'_s = provided area of steel in compression; $A_{s,req}$ = required area of steel in tension; $A'_{s,req}$ = required area of steel in cotmpression; b = distance from bolt centerline to centerline of angle leg; $b' = b - \frac{d_b}{2}$ angle geometrical parameter as defined in AISC *Steel Construction Manual* 14th edition Eq. (9-21) ; c = neutral axis depth; d_b = anchor rod diameter; E_s = steel modulus of elasticity; f'_c = compressive concrete strength; f_u = steel tensile strength; f_y = steel yield strength; F_{nt} = tensile strength of connection (anchor) rods; F_u = specified tensile strength of angle; h = beam height; L_{clear} = clear span of beam between column faces; max. = maximum; M_{des_bot} = design moment creating tension at bottom face of beam

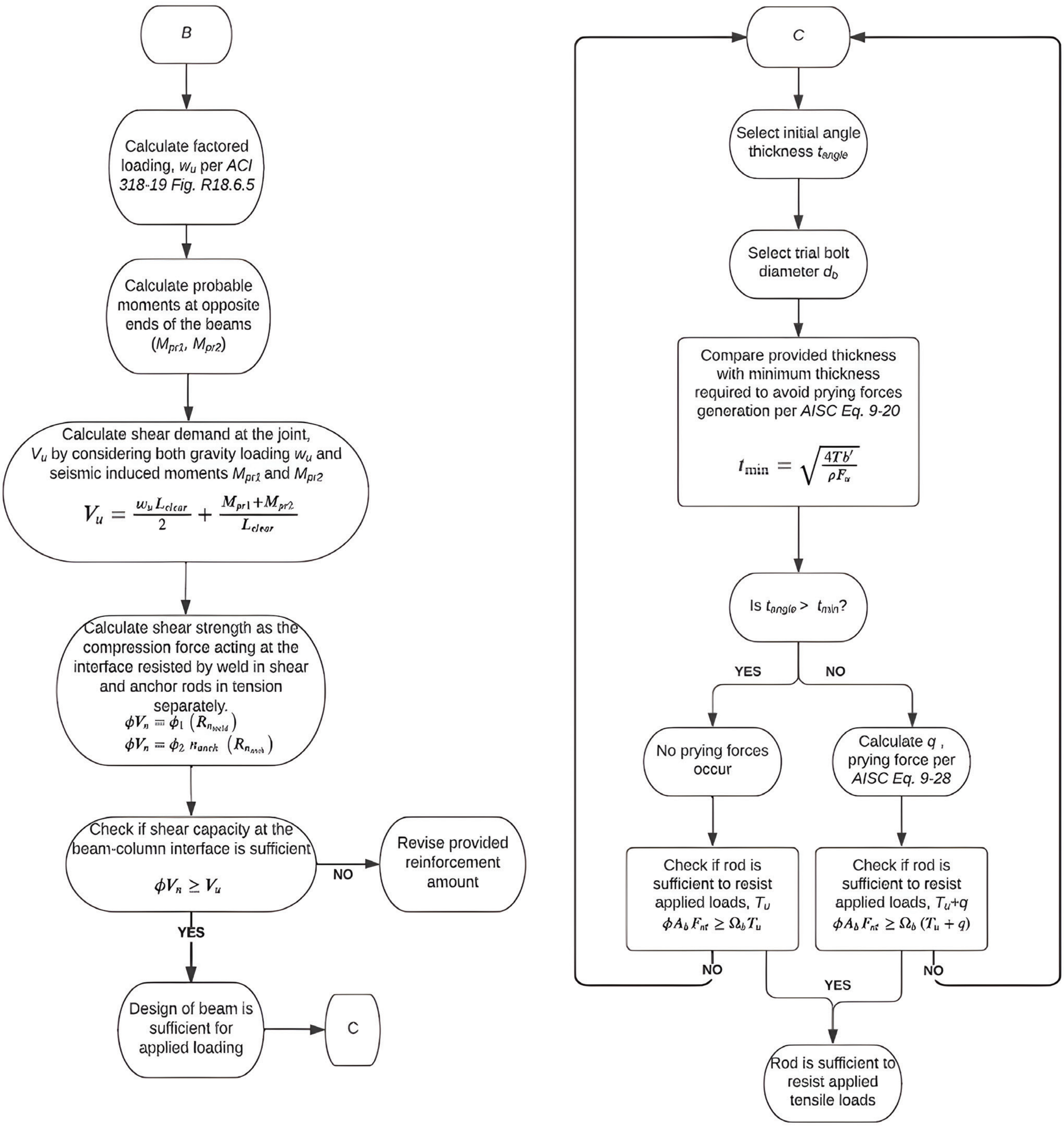

(earthquake loading only); M_{des_top} = design moment due to applied loading (gravity and earthquake loading) creating tension at top face of beam; M_n^+ = positive nominal moment capacity; M_n^- = negative nominal moment capacity; M_{pr1} = probable moment on end 1 of the beam; M_{pr2} = probable moment on end 2 of the beam; min. = minimum; n_{anch} = number of anchors resisting shear at the beam-column interface; q = prying action force; $R_{n_{anch}}$ = anchor rods strength; $R_{n_{weld}}$ = weld strength; t_{angle} = provided angle thickness; t_{min} = angle thickness required to eliminate prying action; T = required strength per bolt; T_u = applied tension force at the angle due to applied gravity and lateral forces; V_n = nominal shear capacity; V_u = maximum applied shear; w_D = applied dead load; w_L = applied live load; w_u = applied factored load; ρ = min (2(b), s), tributary length as described in AISC *Steel Construction Manual* 14th edition Eq. (9-21); ϕ = strength reduction factor; ϕ_1 = strength reduction factor for weld in shear; ϕ_2 = strength reduction factor for anchor rod in tension; Ω_b = overstrength factor of anchor bolts.

(a) $L_{clear} = 15 - (24/12) = 13$ ft (4.0 m)

$L_{clear}/h = ((13)(12))/30 = 5.2 > 4$ **OK**

(b) $L_{clear}/3 = 13/3 = 4.33$ ft (1.32 m) $> h = 30/12 = 2.5$ ft (0.76 m) **OK**

(c) b_b = 16 in. (406 mm) > *MIN* (0.3h = 9 in. [229 mm], 10 in. [254 mm]) = 9 in. (229 mm) **OK**
Selected beam section dimensions are satisfactory.

(d) Estimate the required area of steel reinforcement

$$A_s \geq A_{s,req} = \frac{M_{s,des}}{0.9hf_y} = \frac{(500)(12)}{(0.9)(30)(60)} = 3.7 \text{ in.}^2$$

where

A_s = provided area of steel in tension

Provide three no. 8 beam longitudinal bars and four no. 8 Z-shaped bars, and use 2.5 in. concrete cover d''.

$A_s = (7)(0.79) = 5.53$ in.^{2} $> A_{s,req} = 3.7$ in.^{2} (2400 mm^2)

4. Check that the provided reinforcement satisfies maximum and minimum limitations per ACI 318-19 section 218.6.3.20.025.

$A_s = 5.53$ in.$^2 \leq (0.025)b_b d_b = (0.025)(16)(27.5)$ = 11 in.^{2} (7100 mm^2) **OK**

$$A_s = 5.53 \text{ in.}^2 \geq \frac{200b_d d_b}{f_y} = \frac{(200)(16)(27.5)}{60{,}000}$$

$$= 1.47 \text{ in.}^2 \left(900 \text{ mm}^2\right) \quad \textbf{OK}$$

5. Calculate internal forces.

$A'_s = A_s = 5.53$ in.^{2} (3570 mm^2)

$T_s = A_s f_y = (5.53)(60) = 331.8$ kip (1476 kN)

$C_s = A'_s f_y = (5.53)(60) = 331.8$ kip (1476 kN)

6. Compute β_1.

For $f'_c = 4$ ksi (27.6 MPa), use $\beta_1 = 0.85$.

7. Compute concrete compression force.

$C_c = 0.85 f'_c \beta_1 c b_b = (0.85)(4)(0.85)(c)(16) = 46.24c$

8. Compute the neutral axis depth using equilibrium of internal forces and calculate the depth of the stress block.

$T_s = C_c$

$$c = \frac{T}{46.24} = \frac{331.8}{46.24} = 7.18 \text{ in. } (182 \text{ mm})$$

$a = \beta_1 c = (0.85)(7.18) = 6.1$ in. (155 mm)

9. Compute nominal moment strength.

$C_c = (46.24)(7.18) = 332$ kip (1476.81 kN)

$$M_n = T\left(d_b - \frac{a}{2}\right) = (331.8)\left(27.5 - \frac{6.1}{2}\right) = 676 \text{ kip-ft } (917 \text{ kN-m})$$

10. Check whether ultimate moment capacity is greater than the design moment.

$\phi M_n = (0.9)(676) = 608.5$ kip-ft (825.0 kN-m) $\geq M_{des\_top} = M_{des\_EQ} + M_{des\_DL} = 500$ kip-ft (678 kN-m)

$\phi M_n = (0.9)(676) = 608.5$ kip-ft (825.0 kN-m) $\geq M_{des\_bot} = M_{des\_DL} = 300$ kip-ft (407 kN-m) **OK**

11. Verify that the section is tension controlled.

$$\varepsilon_t = 0.003\left(\frac{d_b}{c} - 1\right) = 0.003\left(\frac{27.5}{4.45} - 1\right) = 0.015 > 0.005 \quad \textbf{OK}$$

$\varepsilon_t \geq 0.004$ **OK**

12. Calculate shear demands due to gravity loads and seismic-induced moments.

$w_u = 1.2w_D + 1.0w_L = (1.2)(2.5) + (1)(1.7) = 4.7$ kip/ft (69 kN/m)

$$M_{pr1} = M_{pr2} = 1.25\left(A_s f_y\left(d - \frac{a}{2}\right) - A'_s f_y\left(d' - \frac{a}{2}\right)\right)$$

= 605.13 kip-ft (820 kN-m)

$$V_u = \frac{w_u L_{clear}}{2} + \frac{M_{pr1} + M_{pr2}}{L_{clear}} = \frac{(4.7)(13)}{2} + \frac{(605.13)(2)}{13}$$

= 123.65 kip (550.0 kN)

13. Select a trial rod diameter.

$d_r = 1.41$ in.

14. Calculate shear capacity at the beam-column interface and check whether it is sufficient. This force is resisted by the weld and the anchor rods connecting the angles to the column and is calculated using parameters as defined in AISC.

$\phi R_n = \phi R_{n_{weld}} = \phi(0.6 \times F_{nw} \times A_{nw}) = (0.75)(0.6)(70)(5) = 158$ kip (703 kN) $> V_u = 123.65$ kip (550 kN) **OK**

where

A_{nw} = effective area of the weld.

F_{nw} = nominal stress of weld material, 70ksi electrode.

$\phi R_n \quad = \phi R_{n_{anch}} = \phi(R_n \times A_b \times n_b) = (0.75)(90)(1.56)(2)$
$= 210.6$ kip (936.7 kN) $> V_u = 123.65$ kip (550 kN) **OK**

where

n_b = number of bolts

15. Select a trial angle thickness.

$t_{angl} = 0.5$ in. (12.7 mm)

16. Calculate total tensile forces in the bolt, including prying forces, if applicable. (They are not applicable in this example because sufficient angle thickness has been provided.)

17. Determine the tensile capacity of the connection rods and whether it is sufficient to resist the maximum tensile loads considering applied tension load due to maximum pull and push forces at the beam tip.

$\phi R_n = \phi A_b F_{nt} = (0.75)((3.14)(0.705)2)(90) = 105.4$ kip (468.8 kN)

$$T_u = \frac{\max(F_{pull}, F_{push})\dfrac{L_{clear}}{d_b}}{n_b} = \frac{(8.51)\dfrac{(13)(12)}{27}}{2} = 24.14 \text{ kip } (107.4 \text{ kN})$$

Q = 3.2 kip (14.2 kN) (calculated using AISC *Steel Construction Manual* Eq. [9-28] and [9-29])

$R_u = \Omega_b(T_u + q) = (3)(27.8) = 83.35$ kip (370.7 kN)

where

R_u = maximum applied tension force

$\phi R_n > R_u$ **OK**

Conclusion

A detailed experimental and numerical study was performed to predict the behavior and investigate the performance of moment-resisting precast concrete beam-column connections under cyclic loading. The proposed FEA methodology was validated against experimental results for one monolithic beam-to-column connection and various novel configurations of precast concrete beam-to-column connections under cyclic loading. Simple detailing modifications resulted in improvements in the performance of the precast concrete connection in terms of strength, stiffness, and energy-dissipation characteristics. It is important to note that the presented study is a part of a larger study performed by the same authors and published in previous articles.[9,10] A design procedure was developed based on the investigated limit states of precast concrete connections under cyclic loading, and a design example is shown to illustrate the proposed procedure.

References

1. Park, R. 1995. "A Perspective on the Seismic Design of Precast Concrete Structures in New Zealand." *PCI Journal* 40 (3): 40–59. https://doi.org/10.15554/pcij.05011995.40.60.

2. Arslan, M. H., H. H. Korkmaz, and F. G. Gulay. 2006. "Damage and Failure Pattern of Prefabricated Structures after Major Earthquakes in Turkey and Shortfalls of the Turkish Earthquake Code." *Engineering Failure Analysis* 13 (4): 537–557. https://doi.org/10.1016/j.engfailanal.2005.02.006.

3. Priestley, M. J. N., and G. A. MacRae. 1999. "Seismic Tests of Precast Beam-to-Column Joint Subassemblages with Unbonded tendons." *PCI Journal* 41 (1): 64–81. https://doi.org/10.15554/pcij.01011996.64.81.

4. Priestley, M. J. N., S. Sritharan, J. R. Conley, and S. Pampanin. 1999. "Preliminary Results and Conclusions from the PRESSS Five-Story Precast Concrete Test Building." *PCI Journal* 44 (6): 42–67. https://doi.org/10.15554/pcij.11011999.42.67.

5. French, C. W., M. Hafner, and V. Jayashankar. 1989. "Connections between Precast Elements—Failure within Connection Region." *Journal of Structural Engineering* 115 (12): 3171–3192. https://doi.org/10.1061/(ASCE)0733-9445(1989)115:12(3171).

6. French, C. W., O. Amu, and C. Tarzikhan. 1989. "Connections between Precast Elements—Failure Outside Connection Region." *Journal of Structural Engineering* 115 (2): 316-340. https://doi.org/10.1061/(ASCE)0733-9445(1989)115:2(316).

7. Nzabonimpa, J. D., W. Hong, and J. Kim. 2017. "Nonlinear Finite Element Model for the Novel Mechanical Beam-Column Joints of Precast Concrete-Based Frames." *Computers and Structures* 189: 31–48. https://doi.org/10.1016/j.compstruc.2017.04.016.

8. Najafgholipour M. A., S. M. Dehgan, A. Dooshabi, and A. Niroomandi. 2017. "Finite Element Analysis of Reinforced Concrete Beam-Column Connections with Governing Joint Shear Failure Mode." *Latin American Journal of Solids and Structures* 14 (7). https://doi.org/10.1590/1679-78253682.

9. Baran, E., M. Mahamid M. Baran M. Kurtoglu, and I. Torra-Bilal. 2021. "Performance of a Moment Resisting Beam-Column Connection for Precast Concrete Construction." *Engineering Structures* 24: 113005. https://doi.org/10.1016/j.engstruct.2021.113005.

10. Torra-Bilal, I., M. Mahamid, and E. Baran. 2022. "Cyclic Behavior of Beam to Column Connections: An

Experimental and Numerical Investigation." *Structures* 35: 939–957. https://doi.org/10.1016/j.istruc.2021.11.046.

11. ACI (American Concrete Institute). 2019. *Acceptance Criteria for Moment Frames Based on Structural Testing and Commentary (Reapproved 2019).* ACI 374.1-05(19). Farmington Hills, MI: ACI.

12. ACI. 2019. *Building Code Requirements for Structural Concrete (ACI 318-19) and Commentary (ACI 318-19R).* Farmington Hills, MI: ACI.

13. ACI 550.3-13. 2003. *Design Specification for Unboned Post-Tensioned Precast Concrete Special Moment Frames Satisfying ACI 3744.1 and Commentary*. ACI Committee 550.

14. ASCE (American Society of Civil Engineers). 2016. *Minimum Design Loads and Associated Criteria for Buildings and Other Structures*. ASCE/SEI 7-16. Reston, VA: ASCE.

15. AISC (American Institute of Steel Construction). 2010. *Steel Construction Manual*. 14th ed. Chicago, IL: AISC.

Notation

a = stress block depth

A_b = anchor rod area

A_{nw} = effective area of the weld.

A_s = provided area of steel in tension

$A_{s,req}$ = required area of steel in tension

A'_s = provided area of steel in compression

$A'_{s,req}$ = required area of steel in compression

b = distance from bolt centerline to centerline of angle leg

b_b = beam width

b_c = column width

b' = $b - \frac{d_b}{2}$ angle geometrical parameter as defined in AISC *Steel Construction Manual* 14th edition Eq. (9-21)

B = available tension per bolt

c = neutral axis depth

C_c = concrete compression force

C_s = compression steel force

d_{bm} = distance from the compression face to the center of reinforcement

d_b = anchor rod diameter

d_c = column depth

d_{cc} = damage variable for compressive damage

d_t = damage variable for tensile damage

d' = concrete cover

D =service dead load

E_s = steel modulus of elasticity

f'_c = compressive concrete strength

f_y = steel yield strength

f_u = steel tensile strength

F_{nt} = tensile strength of connection (anchor) rods

F_{nw} = nominal stress of weld material, 70 ksi (## XX) electrode

F_{pull} = maximum pull force at beam tip used to obtain tension in the anchors

F_{push} = maximum push force at beam tip used to obtain tension in the anchors

F_u = specified tensile strength of angle

h = beam height

L = service live load

L_{clear} = clear span of beam between column faces

M_{des} = design moment

M_{des_bot} = design moment creating tension at bottom face of beam (earthquake loading only)

M_{des_DL} = maximum design moment due to gravity

M_{des_EQ} = maximum design moment due to earthquake load and gravity

M_{des_top} = design moment due to applied loading (gravity and earthquake loading) creating tension at top face of beam

M_n = nominal moment capacity

M_n^{+} = positive nominal moment capacity

M_n^{-} = negative nominal moment capacity, bottom

M_{pr1} = probable moment on end 1 of the beam

M_{pr2} = probable moment on end 2 of the beam

n_{anch} = number of anchors resisting shear at the beam-column interface

n_b = number of bolts

q = prying action force

R_n = nominal tensile capacity

$R_{n_{anch}}$ = anchor rods strength

$R_{n_{weld}}$ = weld strength

R_u = maximum applied tension force

s = bolt spacing

S = service snow load

S_{Ds} = 5% damped, spectral response acceleration parameter at short periods per the general building code

t = angle thickness as provided

t_{angle} = trial angle thickness

t_c = angle thickness required to develop the available strength of the bolt, with no prying action

t_{min} = angle thickness required to eliminate prying action

T_s = tension steel force

T = required strength/bolt

T_u = applied tension force at the angle due to applied gravity and lateral forces

V_n = nominal shear capacity

$V_{n_{anch}}$ = nominal shear capacity of the connection (anchor) rods

$V_{n_{weld}}$ = nominal shear capacity of the weld

V_u = maximum applied shear

w_D = applied dead load

w_L = applied live load

w_u = applied factored load

α = ratio of the moment at the center of the angle leg thickness to the moment at the bolt line

β_1 = factor relating depth of equivalent compressive stress block to depth of neutral axis

δ = ratio of net length at bolt line to gross length at the face of the leg of angle

ε_t = net tensile strain in extreme layer of longitudinal tension reinforcement

θ_{des} = maximum design drift ratio

ρ = min (2(b), s), tributary length as described in AISC *Steel Construction Manual* 14th edition Eq. (9-21)

ρ_{reinf} = reinforcement ratio

ϕ = strength reduction factor

ϕ_1 = strength reduction factor for weld in shear

ϕ_2 = strength reduction factor for anchor rod in tension

Ω_b = overstrength factor of anchor bolts

Ω_c = overstrength factor of compression steel reinforcement

Ω_t = overstrength factor of tension steel reinforcement

About the authors

Mustafa Mahamid, PhD, SE, PE, FACI, FASCE, FSEI, is an associate research fellow at Technion-Israel Institute of Technology in Haifa, a research associate professor at the University of Illinois Chicago, and a structural engineering consultant for multiple structural engineering firms. He serves on ACI Committees 314 (Simplified Design), 441 (Columns), 352 (Joints), and 315 (Detailing) and is a past chair of ACI Committee 421 (Slabs). His interests are concrete design and seismic behavior of structures.

Ines Torra-Bilal, PhD, PE, is a consulting senior engineer at ComEd in Oak Brook, Ill. She received her BS, MS, and PhD from the University of Illinois Chicago. Her interests include research and failure analysis and the design of different types of structures.

Eray Baran, PhD, is a professor of structural engineering at the Middle East Technical University in Ankara, Turkey. His research interests include moment-resisting connections between precast concrete elements, behavior of steel-concrete composite beams, interface shear behavior in composite precast concrete hollow-core slabs, bond behavior of prestressing strands in steel-fiber-reinforced concrete, and behavior of cold-formed structures.

Abstract

This study investigates the behavior of hybrid beam-column connections with numerous detailing methods to be incorporated into precast concrete moment-resisting frames under simulated reversed cyclic loading, and ultimately develops a design procedure. Seismic performance of moment-resisting precast concrete beam-column connections was investigated through simulated reversed cyclic load tests. In addition, nonlinear finite element analysis (FEA) of typical monolithic and precast concrete connections was carried out using a modified concrete damage plasticity model. Good agreement was achieved between experimental and numerical results, which indicates that the FEA model is capable of capturing failure modes of the investigated precast concrete connections. Simple detailing modifications resulted in major improvements in the performance of connections in terms of load-displacement curves, stiffness, and energy dissipation. Finally, a design procedure was developed for the investigated connections based on failure modes and investigated limit states.

Keywords

Beam-column connection, FEA, moment-resisting connection, nonlinear finite element analysis.

Review policy

This paper was reviewed in accordance with the Precast/Prestressed Concrete Institute's peer-review process. The Precast/Prestressed Concrete Institute is not responsible for statements made by authors of papers in *PCI Journal*. No payment is offered.

Publishing details

This paper appears in *PCI Journal* (ISSN 0887-9672) V. 69, No. 4, July–August 2024, and can be found at https://doi.org/10.15554/pcij69.4-02. *PCI Journal* is published bimonthly by the Precast/Prestressed Concrete Institute, 8770 W. Bryn Mawr Ave., Suite 1150, Chicago, IL 60631.

Reader comments

Please address any reader comments to *PCI Journal* editor-in-chief Tom Klemens at tklemens@pci.org or Precast/Prestressed Concrete Institute, c/o *PCI Journal*, 8770 W. Bryn Mawr Ave., Suite 1150, Chicago, IL 60631.